

RPA-like proteins mediate yeast telomere function

Hua Gao^{1,2}, Rachel B Cervantes¹, Edward K Mandell^{1,3}, Joel H Otero³ & Victoria Lundblad¹

Cdc13, Stn1 and Ten1 are essential yeast proteins that both protect chromosome termini from unregulated resection and regulate telomere length. Cdc13, which localizes to telomeres through high-affinity binding to telomeric single-stranded DNA, has been extensively characterized, whereas the contribution(s) of the Cdc13-associated Stn1 and Ten1 proteins to telomere function have remained unclear. We show here that Stn1 and Ten1 are DNA-binding proteins with specificity for telomeric DNA substrates. Furthermore, Stn1 and Ten1 show similarities to Rpa2 and Rpa3, subunits of the heterotrimeric replication protein A (RPA) complex, which is the major single-stranded DNA-binding activity in eukaryotic cells. We propose that Cdc13, Stn1 and Ten1 function as a telomere-specific RPA-like complex. Identification of an RPA-like complex that is targeted to a specific region of the genome suggests that multiple RPA-like complexes have evolved, each making individual contributions to genomic stability.

Telomeres are essential for genomic stability and long-term cellular proliferation. At an organismal level, telomere dysfunction contributes to effects on longevity and age-related phenotypes as well as making pivotal contributions to oncogenesis^{1,2}. To avoid such consequences, two processes must function. First, in cells that depend on continuous proliferation, there must be a mechanism to ensure that the G-rich telomeric tract is continually replenished, as it would otherwise gradually erode with each cell division. The primary pathway for telomere length maintenance in most organisms relies on the telomerase holoenzyme, which elongates the 3' terminus of the G-rich strand of telomeres³. In the absence of telomerase activity, a progressive decline in telomere length eventually inhibits the proliferative capacity of cells^{4,5}, a phenotype that has been referred to as replicative senescence. In telomerase-expressing cells, a number of factors regulate the telomerase holoenzyme, both positively and negatively, thereby ensuring that telomere length homeostasis is carefully maintained^{6,7}.

Cells must also be able to distinguish natural chromosome termini from newly broken DNA ends. The ends of linear chromosomes are normally masked from the types of events that occur at double-strand breaks, through a poorly understood mechanism often referred to as chromosome end protection or telomere capping^{8,9}. Capping relies on a complex set of interactions between multiple telomere-bound proteins, which function to protect telomeres from the inappropriate action of nucleases, from becoming substrates for end-to-end fusions and from the activation of DNA damage checkpoints that halt cell-cycle progression.

In budding yeast, a central player in both telomere length maintenance and chromosome end protection is the single-stranded telomere-binding protein Cdc13, which localizes to chromosome ends by binding with high affinity to the terminal G-rich single-stranded extension^{10,11}. Cdc13 is crucial for telomere capping, as loss

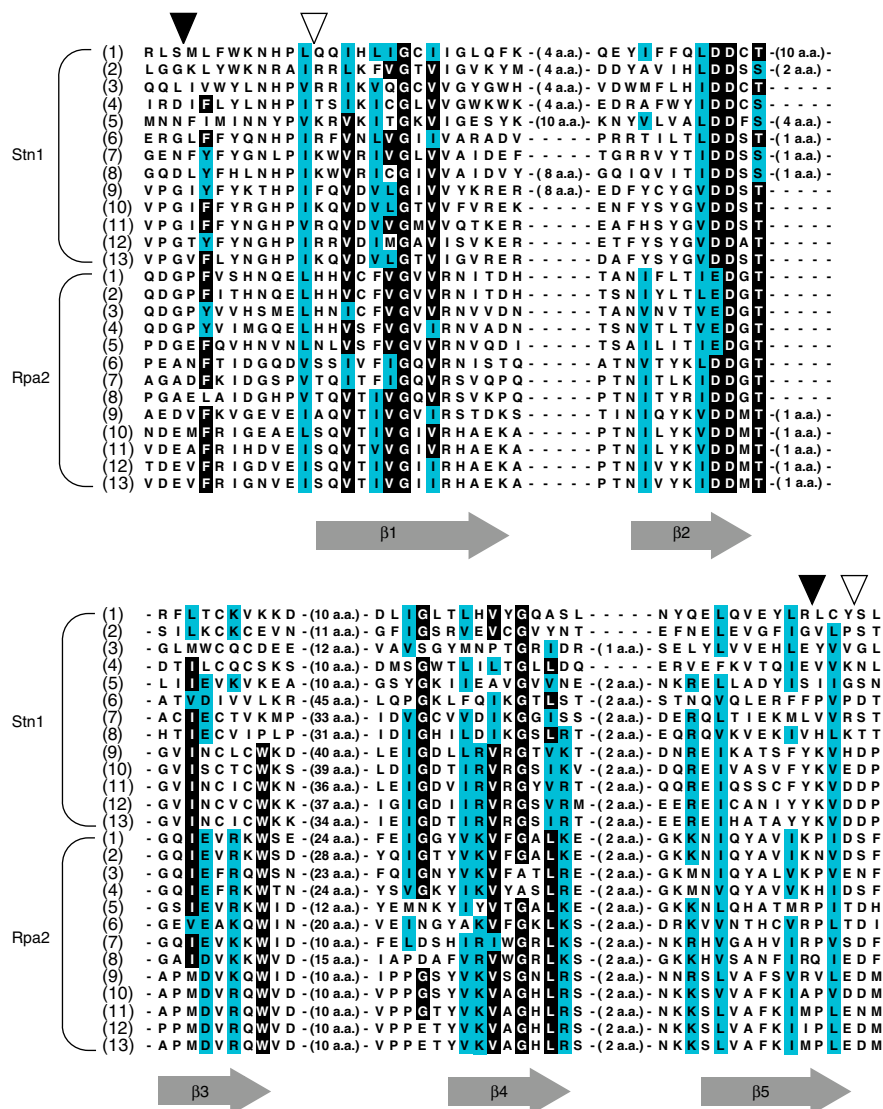
of *CDC13* function exposes chromosome termini to catastrophic resection of the C-strand of telomeres, with the resulting exposed single-stranded region leading to *RAD9*-mediated arrest of the cell cycle^{12,13}. Despite the essential nature of this process, the mechanism by which Cdc13 protects termini from resection is poorly understood, as is the identity of the resecting nuclease(s). Cdc13 also performs a key role in telomere length homeostasis, by recruiting the catalytic core of telomerase to its site of action through a direct interaction between Cdc13 and the Est1 subunit of telomerase^{14–16}. When this interaction fails, because of mutations introduced in either Est1 or Cdc13 that disrupt the binding interface, cells show the same replicative senescence as strains that lack telomerase.

Cdc13 acts at telomeres in collaboration with two less well-characterized proteins, Stn1 and Ten1. Both are novel proteins, with no biochemical activity previously attributed to either. Thus, how these two Cdc13-associated proteins perform their roles at chromosome termini has remained elusive. Like Cdc13, both Stn1 and Ten1 are essential components of the telomere 'cap', as cells depleted for either show the same extensive C-strand degradation and consequent cell-cycle arrest^{17–19}. Furthermore, the lethality of a *cdc13-Δ* null strain can be bypassed if a Stn1-containing complex is ectopically delivered to the telomere¹⁵. Cdc13, Stn1 and Ten1 proteins physically associate with each other, as assessed by both coimmunoprecipitation and two-hybrid assays (refs. 17,18 and R.B.C. and V.L., unpublished data), indicating that these three proteins function at chromosome ends as a heterotrimeric complex. In addition to helping to maintain the telomere cap, this complex also negatively regulates telomere length homeostasis, as revealed by the extensive telomere elongation that occurs in strains bearing certain mutations in each of these three subunits^{17,18,20}. Collectively, these observations indicate that the Cdc13–Stn1–Ten1 complex orchestrates a number of

¹The Salk Institute for Biological Studies, 10010 North Torrey Pines Road, La Jolla, California 92037, USA. ²Department of Biochemistry and Molecular Biology and ³Graduate Program in Cell and Molecular Biology, Baylor College of Medicine, One Baylor Plaza, Houston Texas 77030, USA. Correspondence should be addressed to V.L. (lundblad@salk.edu).

Received 25 October 2006; accepted 22 January 2007; published online 11 February 2007; doi:10.1038/nsmb1205

Figure 1 Stn1 is an OB fold-containing protein. Shown is an alignment of the OB fold of Rpa2 (ref. 25) with an the proposed OB-fold domain of Stn1; residues 59–164 and 55–160 are shown for the *S. cerevisiae* Stn1 and Rpa2 proteins, respectively. The 13 Stn1 and Rpa2 proteins shown were selected from a larger alignment of 26 Stn1 and Rpa2 proteins. Alignments of the two protein families were constructed independently, and the two alignments were then coaligned, guided by results from structure prediction programs (see Methods for more details). Vertical arrowheads indicate the boundaries of a subset of the 11 Rpa2-OB^{Stn1} chimera proteins tested for the ability to rescue the lethality of an *rpa2-Δ* strain (the boundaries for the additional chimeras extend beyond the alignment depicted here); filled arrowheads mark the boundaries of the chimera used in **Figure 2e**. (1) *S. cerevisiae*, (2) *Candida glabrata*, (3) *Ashbya gossypii*, (4) *Kluyveromyces lactis*, (5) *Debaryomyces hansenii*, (6) *Aspergillus nidulans*, (7) *Gibberella zeae*, (8) *Neurospora crassa*, (9) *Danio rerio*, (10) *Xenopus tropicalis*, (11) *Gallus gallus*, (12) *Mus musculus*, (13) *Homo sapiens*.



interactions to promote both telomere capping and telomere length homeostasis, thereby ensuring genome stability.

Another heterotrimeric complex that also binds with high affinity to single-stranded DNA is the RPA complex. RPA, which is often equated with the prokaryotic single-strand binding (SSB) protein, is the major single-stranded DNA-binding activity in eukaryotic cells, with multiple roles in eukaryotic DNA replication, repair and recombination^{21,22}. This complex is composed of multiple oligosaccharide/oligonucleotide-binding (OB) folds, distributed among all three subunits, which are used for both DNA and protein recognition²³. Once bound to DNA, RPA directs subsequent activities, as a consequence of the regulated interaction between RPA and a diverse array of protein complexes involved in DNA metabolism. Owing to the central role of RPA in many DNA transactions, this complex is pivotal in promoting genome stability.

We set out to investigate the potential similarities between these two heterotrimeric single-stranded DNA-binding complexes. We show here that Stn1 and Ten1 have several notable similarities to Rpa2 and Rpa3, the middle and small subunits, respectively, of the RPA complex. In addition, both Stn1 and Ten1 are DNA-binding proteins that, like Cdc13, have a preference for telomeric substrates. We propose that Cdc13, Stn1 and Ten1 form an RPA-like complex that contributes to maintenance of chromosome ends, through mechanisms that may be analogous to those by which the conventional RPA complex functions elsewhere in the genome.

RESULTS

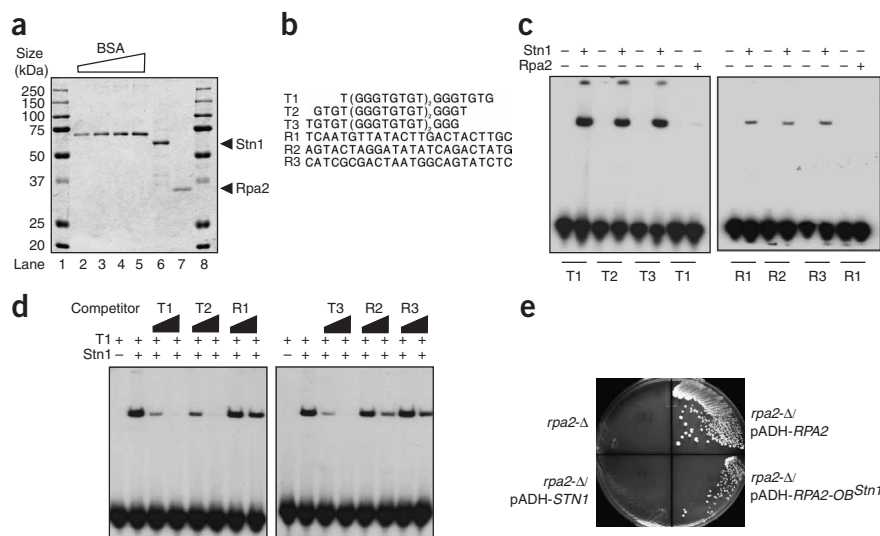
Stn1 and Ten1 are telomere DNA-binding proteins

To uncover possible structural motifs in Stn1 that might provide insight about the function of this protein, an alignment of the

N-terminal portion of 15 Stn1 protein sequences was used as a seed for the structure prediction program HHpred²⁴. HHpred creates a hidden Markov model (HMM) profile from such an alignment and compares this profile to a database of HMM profiles for known structures. In a search of a database of HMM profiles for structures found in the Protein Data Bank, the OB fold of human RPA2 (ref. 25) was the top-ranked hit, with an *E*-value of 9×10^{-10} and a probability score of 97.7. Furthermore, when the N-terminal region of individual Stn1 protein sequences was used as input in the structure-prediction metaserver 3D-Jury²⁶, the OB fold of the human RPA2 protein was again the highest-scoring hit. An alignment between these two protein families was constructed, based on a consensus between the alignments provided by the structure prediction programs HHpred and 3D-Jury (see Methods for more details). The comparison between Rpa2 and Stn1 sequences demonstrates notable sequence conservation that is shared between these two sets of proteins (Fig. 1), which coincides with the previously characterized OB-fold domain of Rpa2 (ref. 25). OB folds are notorious for the absence of primary sequence features that can be used to predict this domain^{27–29}, which further underscores the statistical significance of the sequence similarity between the Stn1 and Rpa2 proteins.

Figure 2 The yeast Stn1 protein binds with enhanced specificity to telomeric substrates.

(a) Flag-Stn1 (lane 6) and Flag-Rpa2 (lane 7), expressed and affinity-purified from *E. coli* from pVL2848 and pVL2941, respectively, and visualized by Coomassie blue staining after 8% (w/v) SDS-PAGE; 0.3, 0.4, 0.5 and 0.6 μ g BSA (lanes 2–5) were used to estimate the concentration of Stn1 and Rpa2. Western analysis with antibody to Flag confirmed the identity of the Stn1 and Rpa2 proteins (data not shown). (b) Sequences of the panel of three telomeric and three random-sequence oligomers used throughout this study; each is 24 nucleotides long. T3 is identical to the substrate used to initially monitor Cdc13 binding¹⁰. (c) Gel mobility shift assay. Flag-Stn1 or Flag-Rpa2 (~550 nM) was incubated with 250 pM radiolabeled telomeric (T1–T3) or random sequence (R1–R3) oligomers. (d) Competition assay. Flag-Stn1 (~300 nM) was incubated with 250 pM radiolabeled telomeric T1 oligomer and a 20- or 200-fold excess of unlabeled competitor oligomers, as indicated. (e) A chimeric Rpa2-OB^{Stn1} protein can function in the place of *RPA2*. Growth of an *rpa2*- Δ strain (YVL2924) bearing either an empty vector (pVL399), or plasmids expressing Stn1, Rpa2 or the Rpa2-OB^{Stn1(62–159)} chimeric protein (pVL1131, pVL3016 or pVL3017, respectively), after eviction of an *RPA2* plasmid (pVL2896). Results are shown with proteins expressed by the *ADH* promoter from high-copy plasmids; however, the Rpa2-OB^{Stn1(62–159)} chimeric protein was also capable of maintaining an *rpa2*- Δ strain, although at slightly reduced efficiency, when expressed by the native *RPA2* promoter from a single-copy plasmid (data not shown). A second chimera (Rpa2-OB^{Stn1(62–163)}) also rescued *rpa2*- Δ , in both high and low copy, also at somewhat reduced efficiency.



This observation suggests that, like the OB fold in Rpa2, the proposed OB fold in Stn1 might be used to contact DNA. To test this, we expressed and purified recombinant Stn1 protein, bearing a single Flag epitope on the N terminus, from *Escherichia coli* (Fig. 2a) and tested this protein preparation for the ability to bind a panel of six single-stranded 24-nucleotide oligomers. Three substrates corresponding in sequence to the G-rich strand of yeast telomeres (T1, T2 and T3) and three composed of random sequence (R1, R2 and R3) (Fig. 2b) were tested. The Stn1 protein bound all three telomeric single-stranded DNA substrates, whereas barely detectable binding to the three random-sequence oligomers was observed, as assessed by a direct binding assay with each of the six substrates (Fig. 2c). The enhanced affinity for telomeric substrates was further confirmed by a competition assay, in which binding of Stn1 to the T1 telomeric oligomer, in the presence of a 20- or 200-fold excess of random or telomeric oligomers, was examined (Fig. 2d). Binding to the T1 substrate was substantially inhibited by a 20-fold excess of any of

the three telomeric oligomers, whereas only modest inhibition was observed even with a 200-fold excess of the three random oligomers. As predicted by the alignment in Figure 1, this DNA-binding activity mapped to the proposed OB fold domain of Stn1, as Flag-Stn1_{64–199} bound a single-stranded telomeric DNA substrate with an affinity that was comparable to that of the full-length Stn1 protein (Supplementary Fig. 1 online). These observations show that Stn1 is a telomere-specific DNA-binding protein, contacting DNA through an OB fold-like domain that shows sequence similarity to the structurally characterized OB fold of Rpa2.

As a further test of the potential parallels between Stn1 and Rpa2, we performed a domain swap between these two proteins, replacing the OB-fold domain of Rpa2 with the comparable region of the Stn1 protein. Notably, two Rpa2-OB^{Stn1} chimeras rescued the inviability of an *rpa2*- Δ yeast strain (Fig. 2e and data not shown). In contrast, the *rpa2*- Δ strain could not be rescued by high-level expression of the full-length Stn1 protein (Fig. 2e), and these two Rpa2-OB^{Stn1} proteins did

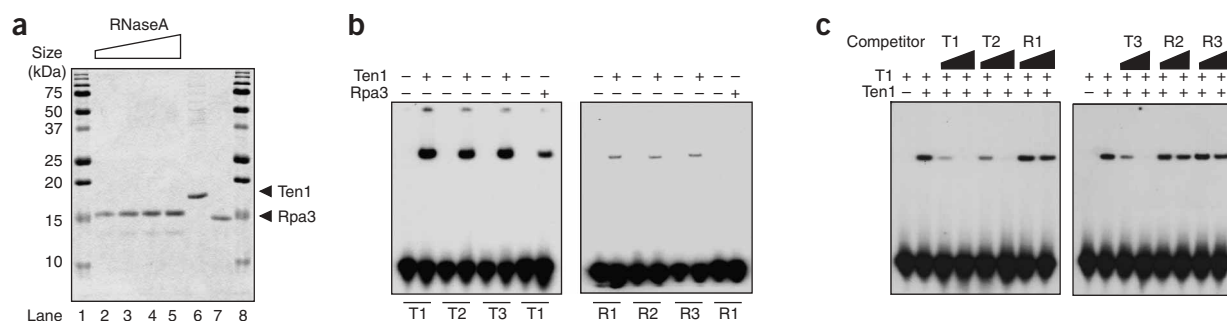


Figure 3 Ten1 binds telomeric DNA sequence-specifically. (a) Ten1-Flag (lane 6) and Rpa3-Flag (lane 7) were expressed from pVL2933 and pVL2942, respectively, affinity-purified from *E. coli*, resolved by 15% (w/v) SDS-PAGE and visualized by Coomassie blue staining; 0.3, 0.4, 0.5 and 0.6 μ g RNase A (lanes 2–5) were used to estimate protein concentration of Ten1 and Rpa3. (b) Gel mobility shift assay. Ten1-Flag or Rpa3-Flag (both at ~1.2 μ M) was incubated with 250 pM radiolabeled oligomers, using the same substrates and conditions as in Figure 2. (c) Competition assay. Ten1-Flag (~600 nM) was incubated with 250 pM radiolabeled telomeric T1 oligomer and a 20- or 200-fold excess of unlabeled competitor oligomers, as indicated.

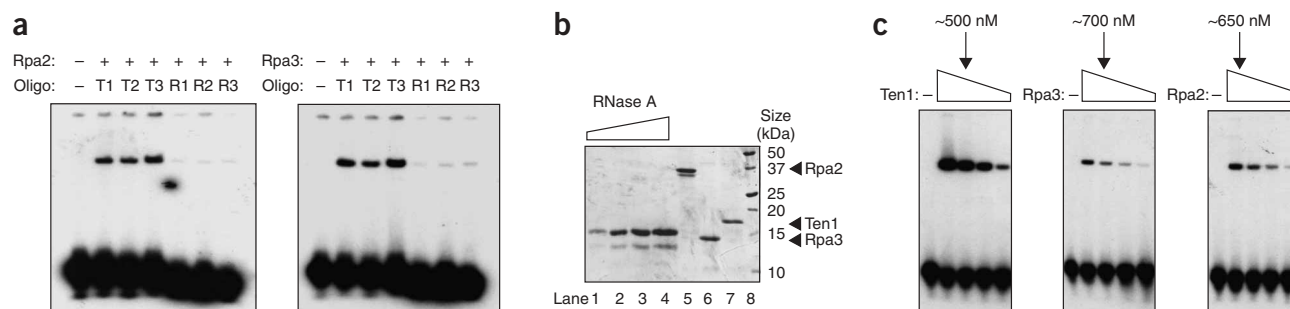


Figure 4 Rpa2 and Rpa3 interact weakly with telomeric substrates. **(a)** Gel mobility shift assay. Flag-Rpa2 or Rpa3-Flag (~730 nM) was incubated with 250 pM radiolabeled oligomers, using the same substrates and conditions as in **Figure 2**. Rpa2 and Rpa3 protein preparations were the same as in **Figure 2a** and **Figure 3a**, respectively. **(b)** Flag-Rpa2 (lane 5), Rpa3-Flag (lane 6) and Ten1-Flag (lane 7) were affinity-purified from *E. coli* and visualized by Coomassie blue staining after 15% (w/v) SDS-PAGE. Lanes 1–4 contain 0.2, 0.5, 1.0 and 1.5 μ g RNase A. **(c)** Gel mobility shift assay. Two-fold dilution series of Ten1, Rpa3 or Rpa2 was incubated with the telomeric substrate T3 (125 pM). Protein concentrations indicated are based on comparison with RNase A standards in **b**.

not rescue a *stn1- Δ* strain (data not shown). The OB fold of Rpa2 has previously been shown to be essential for viability^{30–32}. Thus, the viability of the *rpa2- Δ* strain expressing the Rpa2-OB^{Stn1} chimeric protein demonstrates that the essential function(s) of RPA2 that reside within this domain can be restored by substituting the OB fold of Rpa2 with the comparable region of the Stn1 protein. This not only provides further support for the premise that the N-terminal domain of Stn1 contains an OB fold, it also extends the biochemical comparison (and perhaps reveals an evolutionary relationship) between Stn1 and Rpa2.

In addition, we tested whether the Ten1 protein also bound single-stranded DNA substrates. Recombinant Ten1-Flag was expressed and affinity-purified from *E. coli* (**Fig. 3a**) and tested for binding to the same panel of DNA oligomers (**Fig. 2b**) that were used to test Stn1 binding. Notably, the Ten1 protein also bound the panel of three telomeric oligomers but showed greatly reduced binding to random-sequence oligomers, as determined by both a direct binding assay (**Fig. 3b**) and a competition assay (**Fig. 3c**). Thus, like Stn1, Ten1 showed specificity for telomeric substrates. The relative affinity of Ten1 for DNA was weaker, however, as binding of Ten1 to a telomeric substrate was reduced, compared with the activity of Stn1_{64–199} or the full-length Stn1 protein with the same substrate (**Supplementary Fig. 1** and data not shown).

The above experiments, combined with previous observations about the Cdc13 protein, demonstrate that Cdc13, Stn1 and Ten1 each bind DNA, with a graded specificity for telomeric substrates. Furthermore, both Cdc13 (ref. 33) and Stn1 (**Figs. 1** and **2**) use OB folds that are related to the comparable folds in Rpa1 and Rpa2, respectively. Cdc13 is presumably the primary factor dictating localization of this complex to chromosome ends, as Cdc13 binds with exceptionally high affinity to telomeric DNA¹⁰. However, the preference of Stn1 and Ten1 for telomeric substrates suggests that these two proteins may also contribute to the association of this complex with chromosome termini.

Rpa2 and Rpa3 weakly bind telomeric substrates

In the experiments shown in **Figures 2** and **3**, recombinant Flag-Rpa2 and Rpa3-Flag proteins were also affinity-purified from *E. coli* and tested for DNA binding, in parallel with Stn1 and Ten1. Unexpectedly, we detected weak binding by the Rpa3 protein to the single-stranded T1 telomeric oligomer, whereas no binding to the random-sequence R1 oligomer was observed (**Fig. 3b**). Similarly, extended exposure of

the experiment shown in **Figure 2c** revealed a weak interaction between Rpa2 and the T1 telomeric substrate. These observations were somewhat surprising, as the Rpa2 and Rpa3 subunits have not been observed to bind single-stranded DNA when tested as individual purified proteins in similar gel-shift assays^{31,34}. Furthermore, previous studies have suggested that the subunits of this complex bind relatively nonspecifically to single-stranded DNA, although the intact complex shows some preference for pyrimidine-rich substrates (reviewed in ref. 21).

To explore this in more detail, we examined the purified Rpa2 and Rpa3 proteins for binding to the panel of three telomeric and three random-sequence oligomers. Both proteins show the same relative pattern of specificity of binding to these six substrates as Stn1 and Ten1. Rpa2 and Rpa3 each showed weak, but detectable, binding to each of the G-rich telomeric DNAs, but greatly reduced binding to the three random-sequence substrates (**Fig. 4a**). R1 and R3 are considerably more pyrimidine-rich than the three telomeric oligomers; thus, the enhanced binding to T1, T2 and T3 cannot be attributed to the previously observed preference of the intact RPA complex for pyrimidine-containing substrates. The apparent affinity of Rpa2 and Rpa3 for these telomeric substrates was clearly reduced, however, as revealed by a second experiment that directly compared binding of Ten1, Rpa2 and Rpa3 to the same telomeric oligomer (**Fig. 4b,c**).

Stn1 and Ten1 form a subcomplex

Rpa2 and Rpa3 can form a soluble subcomplex *in vitro*, either between the two full-length proteins or between Rpa3 and the OB fold of Rpa2 (refs. 34,35). Stn1 and Ten1 have also been previously reported to interact, as assessed by coimmunoprecipitation from yeast extracts and two-hybrid assays^{17,18} (see also **Supplementary Fig. 2** online). As neither of these approaches addressed the stoichiometry of this association or whether the Stn1-Ten1 interaction was direct, we examined whether the Stn1 and Ten1 proteins could form a complex *in vitro*. Flag-Stn1 and untagged Ten1 were expressed in a coupled transcription-translation reaction in rabbit reticulocyte lysates as ³⁵S-labeled proteins, either separately or in combination (in the latter case, the Ten1 protein was expressed in excess, relative to Stn1; lane 3 of **Fig. 5a**). After anti-Flag immunoprecipitation and SDS-PAGE, the relative proportions of [³⁵S]Flag-Stn1 and [³⁵S]Ten1 were quantified. The untagged Ten1 cofractionated with Flag-Stn1, forming a complex with roughly 1:1 stoichiometry (**Fig. 5a**, lane 6).

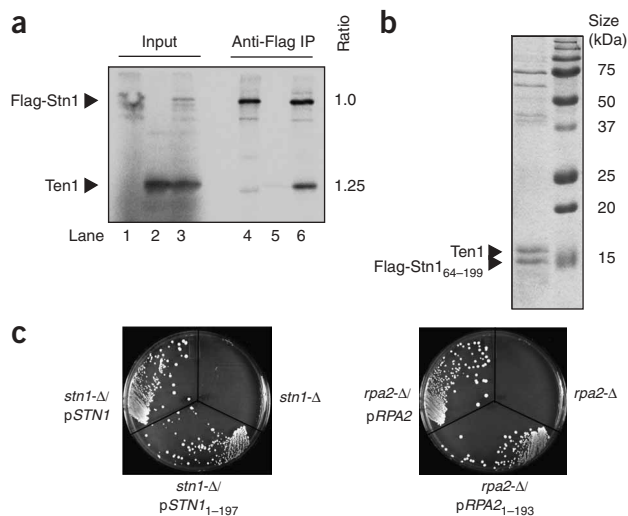


Figure 5 Stn1 and Ten1 form a subcomplex analogous to the Rpa2–Rpa3 subcomplex. **(a)** Ten1 copurifies with the full-length Stn1 protein. Flag-Stn1 and Ten1 were translated from pVL2848 and pVL3115, respectively, in a coupled transcription-translation reaction with [³⁵S]methionine as the only source of methionine, either separately (lanes 1 and 2, respectively) or together (lane 3, with Ten1 in approximately five- to ten-fold excess). Aliquots from these three translation reactions were immunoprecipitated (IP) with antibody to Flag, and immunoprecipitates were resolved on a 15% (w/v) SDS-PAGE gel (lanes 4–6). Stn1 and Ten1 protein signals in lane 6 were quantified by PhosphorImager analysis; indicated ratio is normalized for the number of [³⁵S]methionine residues in each protein. **(b)** Ten1 copurifies with the OB fold of Stn1. Flag-Stn1_{64–199} was coexpressed with Ten1 in *E. coli* from pVL3066. Flag-containing complexes were bound to anti-Flag agarose beads and then eluted with Flag peptide. Identities of the Flag-Stn1_{64–199} and Ten1 protein bands were confirmed by western analysis with antibodies to Flag and Ten1, respectively (data not shown). **(c)** The N-terminal domains of *STN1* and *RPA2* are sufficient for viability. Left, growth of an *stn1-Δ* strain (YVL2394) bearing an empty vector (YCplac111) or plasmids expressing Stn1 or Stn1_{1–197} (pVL1492 or pVL3226, respectively), after eviction of a *STN1* plasmid (pVL1046). Right, growth of an *rpa2-Δ* strain (YVL2924) bearing an empty vector (YCplac111) or plasmids expressing Rpa2 or Rpa2_{1–193} (pVL2894 or pVL3229, respectively), after eviction of an *RPA2* plasmid (pVL2896). All proteins are expressed in single copy, by the native *STN1* or *RPA2* promoter, respectively.

A subcomplex between just the OB-fold domain of Stn1 (Stn1_{64–199}) and the full-length Ten1 protein could also be detected. We prepared extracts from an *E. coli* strain that coexpressed Flag-Stn1_{64–199} and Ten1, subjected the extracts to anti-Flag immunoprecipitation, eluted these immunoprecipitates with Flag peptide and examined the eluates on Coomassie-stained SDS-PAGE gels. Stn1_{64–199} formed a stable complex with the Ten1 protein (Fig. 5b), mimicking the extensively analyzed subcomplex between the Rpa2 OB fold and Rpa3 (refs. 25,34,35).

RPA2 and *STN1* have two additional points of similarity. *In vivo* assembly of the RPA complex relies on independent interactions between Rpa2 and Rpa1 and between Rpa2 and Rpa3, as Rpa1 and Rpa3 interact in a two-hybrid assay only when Rpa2 is overexpressed³⁶. Similarly, both Cdc13 and Ten1 associate with Stn1, but not with each other, when examined in a two-hybrid test (Supplementary Fig. 2). However, an interaction between Ten1 and Cdc13 can be detected in this assay if the Stn1 protein is simultaneously overexpressed (Supplementary Fig. 2). Thus, like Rpa2, Stn1 acts as a bridge between the other two subunits. Finally, previous work has shown that the essential region of *RPA2* maps to the N-terminal, OB fold-containing domain³¹. We found that plasmids expressing Stn1_{1–197} and Rpa2_{1–193} rescued the lethality of *stn1-Δ* and *rpa2-Δ* strains, respectively (Fig. 5c). Thus, the essential function of *STN1* maps to its N-terminal domain, once again in parallel with what has been observed for *RPA2* (see also Supplementary Fig. 3 online).

DISCUSSION

An emerging theme in chromosome biology has been the discovery of protein complexes that bear striking structural similarities to complexes that are required for canonical semiconservative DNA replication. For example, the Rad9, Hus1 and Rad1 proteins assemble to form a heterotrimeric complex, often referred to as the 9-1-1 complex, that strongly resembles a PCNA-like sliding clamp³⁷. Similarly, the DNA damage response protein Rad17 (Rad24 in budding yeast) is the large subunit of a clamp loader that functions in a manner similar to the canonical replication factor-C (RF-C) clamp loader³⁸. During DNA replication, RF-C mediates loading of PCNA onto DNA, whereas in response to genotoxic stress, the Rad17-containing RF-C-like complex loads the 9-1-1 complex onto DNA, presumably at the sites of DNA damage (reviewed in ref. 39). RF-C-like complexes are not restricted only to DNA damage responses, as additional clamp-

loader-like complexes that contribute to several aspects of genome stability have also been described⁴⁰.

The observations reported in this study suggest yet another example: we propose that the Cdc13, Stn1 and Ten1 proteins form an RPA-like complex that is specifically dedicated to binding chromosome termini. This proposal is based on several points of comparison between subunits of the RPA complex and the Cdc13 complex. Both Cdc13 and Rpa1 bind single-stranded DNA with high affinity, through a centrally located OB-fold domain^{33,41}, which is positioned immediately adjacent to a less well-characterized OB fold located in the C-terminal region of each protein^{42,43}. Furthermore, although these two proteins do not show any detectable sequence similarity, they share a remarkably similar domain architecture (discussed in more detail in Supplementary Fig. 3).

Like Cdc13 and Rpa1, Stn1 and Rpa2 also use OB-fold domains to contact single-stranded DNA. Despite the fact that OB folds are usually characterized by the absence of a primary sequence signature, the Stn1 and Rpa2 protein families share notable protein similarity in their N-terminal domains, with the highest degree of similarity in the β-strands that are the core structural feature of OB-fold domains. This sequence similarity seems to reflect functionally equivalent roles for each protein, according to several lines of evidence. The DNA-binding activity of Rpa2 and Stn1 maps to their respective OB-fold domains, and this domain in each protein is also responsible for contacting Rpa3 and Ten1, respectively. Perhaps the most noteworthy observation supporting the premise that Stn1 and Rpa2 have similar biochemical activities is the ability of the Rpa2-OB^{Stn1} chimera, with its essential OB-fold domain substituted by the comparable region of Stn1, to maintain viability in the absence of the *RPA2* gene. We also attempted to generate a functional reverse chimera (Stn1-OB^{Rpa2}), but were unsuccessful. This failure may be the consequence of the limitations of this particular experiment, as the boundaries of these chimeric proteins seem to be crucial for function (only 2 of 11 Rpa2-OB^{Stn1} candidate chimeras, which differed slightly in the junction of the chimera boundaries, rescued the lethality of an *rpa2-Δ* strain). Alternatively, the inability to generate a functional Stn1-OB^{Rpa2} chimera may reflect a functional difference between Stn1 and Rpa2, such as the enhanced affinity of Stn1 for telomeric DNA.

The very small Ten1 and Rpa3 proteins also share several biochemical features. Both are DNA-binding proteins, with a weak specificity for telomeric substrates, and both proteins can form subcomplexes with full-length Stn1 and Rpa2 proteins, respectively, or with just the OB fold of each. Therefore, Ten1 has two key properties that would be predicted for the smallest subunit of an RPA-like complex. However, we were unable to detect any sequence similarity between the Rpa3 and Ten1 protein families, using the bioinformatics techniques that uncovered similarities between Stn1 and Rpa2. Thus, we were unable to conclude whether Ten1, like Cdc13 and Stn1, contacts DNA through an OB fold. The inability to detect an Rpa3-like OB fold in Ten1 may, however, be a consequence of the poor conservation of both the Ten1 and the Rpa3 protein families at the primary sequence level (see **Supplementary Fig. 3** for more discussion of this point). Therefore, determination of whether Ten1 has an OB fold or not will presumably require a structural approach.

The proposal that Cdc13, Stn1 and Ten1 form a telomere-dedicated RPA-like complex also leads to the prediction that these three proteins should form a stable trimeric complex, with a stoichiometry comparable to that of the canonical RPA complex. Although it is clear that Cdc13, Stn1 and Ten1 physically associate *in vivo*, as assessed by coimmunoprecipitation studies (refs. 17,18 and R.B.C. and V.L., unpublished data), the abundance of this complex in budding yeast is extremely low. This has precluded fractionation of the complex from yeast extracts in sufficient purity to allow an assessment of subunit stoichiometry (an issue that has also plagued analysis of the yeast telomerase holoenzyme complex). We have been also unsuccessful, at least so far, in reconstituting the heterotrimeric complex with recombinant proteins expressed in either *E. coli* or coupled transcription-translation systems (H.G., R.B.C. and V.L., unpublished observations). Additional biochemical approaches will be necessary to address this issue.

The proposal that an RPA-like complex mediates chromosome end protection may further extend a model for newly replicated telomeres that is under consideration by many laboratories. This model is analogous, at least in part, to the initial steps in double-strand break repair, whereby extensive 5' resection of the DNA ends creates single-stranded ends that are bound by RPA, which subsequently recruits checkpoint complexes and other factors that ultimately promote repair of the break^{44,45}. At chromosome ends, a similar 5' resection also occurs immediately after conventional DNA replication: the C-strand of the blunt termini created by leading-strand replication is processed by an as-yet-unidentified nuclease^{46,47}, with the resulting single-stranded G-strand bound by Cdc13 (ref. 11,48) and presumably Stn1 and Ten1. In a manner similar to the conventional RPA, once bound to telomeres, the proposed telomere-dedicated RPA-like complex also recruits additional factors (such as telomerase), although subsequent steps must differ between chromosome termini and double-strand breaks, as these two sets of processing events result in very different outcomes. Thus, the proposal that Cdc13, Stn1 and Ten1 form an RPA-like complex that functions at telomeres provides new insights into the role of these three proteins as well as a framework for a more detailed mechanistic understanding of chromosome end protection.

Finally, in our investigation of potential biochemical similarities between Stn1 and Rpa2 and between Ten1 and Rpa3, we discovered an unexpected specificity of Rpa2 and Rpa3 for telomeric over random sequence substrates. Although RPA has long been presumed to interact with single-stranded DNA in a relatively nonspecific manner, several prior observations have not been entirely consistent with this assumption. For example, in yeast, the RPA complex does in fact

localize to chromosome ends, where it can modulate telomere length regulation^{48–50}. A series of intriguing questions for future studies concerns whether the canonical RPA complex and the proposed telomere-dedicated RPA-like complex intersect, through a direct interaction or by competition for binding sites to mediate single-stranded DNA transactions at telomeres.

METHODS

Strains and plasmids. The isogenic strains YVL2924(*MATa rpa2-Δ::TRP1 ura3-52 lys2-801 trp1-Δ1 his3-Δ200 leu2-Δ1/pCEN URA RPA2*) and YVL2394(*MATa stn1-Δ::KAN ura3-52 lys2-801 trp1-Δ1 his3-Δ200 leu2-Δ1 ade2-101/pCEN URA STN1*) were used in the plasmid shuffle experiments shown in **Figure 2e** and **Figure 5c**, respectively. A list of the plasmids used in this study, as well as the starting vectors used for each set of plasmid constructions, is shown in **Supplementary Table 1** online. Plasmids encoding the Rpa2-OB^{Stn1} fusions were constructed by gap repair in yeast, through cotransformation of pVL2894, digested to create a 110-base-pair gap within the RPA2 gene, and PCR products containing STN1-coding sequences flanked by 45 base pairs of RPA2-coding sequences. Candidate chimeric plasmids were rescued and sequenced before further analysis, and selected chimeras were cloned into pVL399 for overexpression studies.

Protein alignments. The Stn1 and Rpa2 sequences shown in the alignments in **Figure 1** were recovered by HMM searches of a variety of protein and genome databases, as well as iterative position-specific iterated (PSI)-BLAST searches of the nonredundant protein database^{51,52}. Candidate proteins were determined to be Rpa2 or Stn1 homologs if PSI-BLAST searches assigned them an *E*-value ≤ 0.0005 , using full-length Rpa2 protein sequences or the N-terminal OB-fold region of Stn1, respectively. In addition, Rpa2 and Stn1 sequences were included in subsequent analyses only if genes encoding both the full-length protein sequences could be recovered from a given genome. Multiple TCOFFEE- and PROBCONS-generated alignments were used to create full-length alignments using the COMBINE function of the TCOFFEE web server^{53–55}. Alignments of the Rpa2 and Stn1 protein families were generated independently, and the subsequent alignment between the two protein families was based on a consensus between the alignments provided by the structure-prediction programs HHPred and 3D-Jury. Alignment among individual family members was not compromised to improve alignment between the two protein families, with the exception of the third β -sheet in the OB fold of Stn1; the alignment in this poorly conserved region of Stn1 is based on predicted alignment with Rpa2.

Protein expression and affinity purification. The *E. coli* strain BL21(DE3)-pLysS, [F⁻, *ompT hsdSB (r_B m_B) gal dcm* (DE3) pLysS (CamR)] was used for all protein expression and affinity-purification studies. Cultures of *E. coli*, freshly transformed with relevant plasmids, were grown in 150 ml liquid LB medium containing 60 $\mu\text{g ml}^{-1}$ carbenicillin at 37 °C to $A_{600} = 0.6$. IPTG was added to a final concentration of 0.5 mM and cultures were incubated at 26 °C for 3.5 h. Cells were pelleted at 5,000g for 10 min, resuspended in 3 ml of TBS lysis buffer (50 mM Tris-HCl, 150 mM NaCl (pH 7.4), 1% (v/v) Triton X-100, 1 mM EDTA) and sonicated using a Branson Sonifier 450 three times for 30 s each, with a 1-min incubation on ice between each sonication step. Lysates were clarified by centrifuging twice at 21,000 g for 20 min at 4 °C. Packed anti-Flag M2 agarose beads (60 μl ; Sigma) were added to the cleared lysate and rotated for 3 h at 4 °C. Beads were washed three times for 15 min at 4 °C in 1 ml TBS, and bound protein was eluted by incubating beads in 300 μl of 500 ng μl^{-1} Flag peptide (Sigma). Protein concentration was measured against a BSA serial dilution curve on a Coomassie-stained 8% (w/v) SDS-PAGE gel for proteins larger than 50 kDa, or against an RNase A serial dilution curve on a 15% (w/v) SDS-PAGE gel for proteins smaller than 30 kDa. For analysis of proteins expressed in rabbit reticulocyte extracts, pRSET derivatives, as indicated, were added to a 50 μl TNT Quick Coupled Transcription/Translation reaction (Promega) with [³⁵S]Met (Amersham Biosciences) as the sole source of methionine and incubated for 90 min at 30 °C, according to the manufacturer's instructions. TBS lysis buffer (1 ml) and 30 μl packed anti-Flag M2 agarose beads were then added, and samples were processed as described above.

Electrophoretic mobility shift assays. Binding reactions were done in 10 mM HEPES (pH 7.8), 75 mM KCl, 2.5 mM MgCl₂, 0.1 mM EDTA, 1 mM DTT, 3% (v/v) Ficoll and 50 μg ml⁻¹ poly(dI-dC). DNA oligomers were 5' end-labeled with [³²P]dATP by T4 polynucleotide kinase (NEB) and separated from unincorporated activity using a Micro Biospin column (BioRad). For the direct binding assays, affinity-purified proteins and heat-denatured radiolabeled oligomers were added sequentially at 10-min intervals, incubated 20 min at 25 °C, electrophoresed through a 5% (w/v) nondenaturing polyacrylamide gel in 1× TBE at 250 V and analyzed by autoradiography. For competition assays, proteins were incubated with a 20- or 200-fold excess of unlabeled competitor oligomers for 10 min at 25 °C, before the addition of the radiolabeled oligomer, followed by an additional 20-min incubation at 25 °C.

Note: Supplementary information is available on the Nature Structural & Molecular Biology website.

ACKNOWLEDGMENTS

We thank the Brill (Rutgers University), Elledge (Harvard Medical School) and Wold (University of Iowa) laboratories for gifts of strains and plasmids, D. Wuttke and M. Wold for scientific conversations and advice, and E. Ford for technical assistance. This research was supported by Department of Defense postdoctoral fellowship DAMD 17-02-1-0276 (to R.B.C.), by grant GM55867 from the US National Institutes of Health and by the Lebensfeld Foundation.

COMPETING INTERESTS STATEMENT

The authors declare that they have no competing financial interests.

Published online at <http://www.nature.com/nsmb/>

Reprints and permissions information is available online at <http://npg.nature.com/reprintsandpermissions>

- Shay, J.W. & Wright, W.E. in *Telomeres* 2nd edn. (eds. de Lange, T., Lundblad, V. & Blackburn, E.) 81–108 (Cold Spring Harbor Laboratory, New York, 2005).
- Stewart, S.A. & Weinberg, R.A. Telomeres: cancer to human aging. *Annu. Rev. Cell Dev. Biol.* **22**, 531–557 (2006).
- Greider, C.W. & Blackburn, E.H. Identification of a specific telomere terminal transferase activity in *Tetrahymena* extracts. *Cell* **43**, 405–413 (1985).
- Lundblad, V. & Szostak, J.W. A mutant with a defect in telomere elongation leads to senescence in yeast. *Cell* **57**, 633–643 (1989).
- Bodnar, A.G. *et al.* Extension of life-span by introduction of telomerase into normal human cells. *Science* **279**, 349–352 (1998).
- Smogorzewska, A. & de Lange, T. Regulation of telomerase by telomeric proteins. *Annu. Rev. Biochem.* **73**, 177–208 (2004).
- Hug, N. & Lingner, J. Telomere length homeostasis. *Chromosoma* **115**, 413–425 (2006).
- Blackburn, E.H. Telomere states and cell fates. *Nature* **408**, 53–56 (2000).
- de Lange, T. Shelterin: the protein complex that shapes and safeguards human telomeres. *Genes Dev.* **19**, 2100–2110 (2005).
- Nugent, C.I., Hughes, T.R., Lue, N.F. & Lundblad, V. Cdc13p: a single-strand telomeric DNA-binding protein with a dual role in yeast telomere maintenance. *Science* **274**, 249–252 (1996).
- Taggart, A.K., Teng, S.C. & Zakian, V.A. Est1p as a cell cycle-regulated activator of telomere-bound telomerase. *Science* **297**, 1023–1026 (2002).
- Weinert, T.A. & Hartwell, L.H. Cell cycle arrest of *cdc* mutants and specificity of the *RAD9* checkpoint. *Genetics* **134**, 63–80 (1993).
- Garvik, B., Carson, M. & Hartwell, L. Single-stranded DNA arising at telomeres in *cdc13* mutants may constitute a specific signal for the *RAD9* checkpoint. *Mol. Cell. Biol.* **15**, 6128–6138 (1995).
- Evans, S.K. & Lundblad, V. Est1 and Cdc13 as comediators of telomerase access. *Science* **286**, 117–120 (1999).
- Pennock, E., Buckley, K. & Lundblad, V. Cdc13 delivers separate complexes to the telomere for end protection and replication. *Cell* **104**, 387–396 (2001).
- Bianchi, A., Negrini, S. & Shore, D. Delivery of yeast telomerase to a DNA break depends on the recruitment functions of Cdc13 and Est1. *Mol. Cell* **16**, 139–146 (2004).
- Grandin, N., Reed, S.I. & Charbonneau, M. Stn1, a new *Saccharomyces cerevisiae* protein, is implicated in telomere size regulation in association with Cdc13. *Genes Dev.* **11**, 512–527 (1997).
- Grandin, N., Damon, C. & Charbonneau, M. Ten1 functions in telomere end protection and length regulation in association with Stn1 and Cdc13. *EMBO J.* **20**, 1173–1183 (2001).
- Vodenicharov, M.D. & Wellinger, R.J. DNA degradation at unprotected telomeres in yeast is regulated by the CDK1 (CDC28/Clb) cell cycle kinase. *Mol. Cell* **24**, 127–137 (2006).
- Chandra, A., Hughes, T.R., Nugent, C.I. & Lundblad, V. Cdc13 both positively and negatively regulates telomere replication. *Genes Dev.* **15**, 404–414 (2001).
- Wold, M.S. Replication Protein A: a heterotrimeric, single-stranded DNA-binding protein required for eukaryotic DNA metabolism. *Annu. Rev. Biochem.* **66**, 61–92 (1997).
- Iftode, C., Daniely, Y. & Borowiec, J.A. Replication Protein A (RPA): the eukaryotic SSB. *Crit. Rev. Biochem. Mol. Biol.* **34**, 141–180 (1999).
- Bochkarev, A. & Bochkareva, E. From RPA to BRCA2: lessons from single-stranded DNA binding by the OB-fold. *Curr. Opin. Struct. Biol.* **14**, 36–42 (2004).
- Soding, J., Biegert, A. & Lupas, A.N. The HHpred interactive server for protein homology detection and structure prediction. *Nucleic Acids Res.* **33**, W244–W248 (2005).
- Bochkarev, A., Bochkareva, E., Frappier, L. & Edwards, A.M. The crystal structure of the complex of Replication Protein A subunits RPA32 and RPA14 reveals a mechanism for single-stranded DNA binding. *EMBO J.* **18**, 4498–4504 (1999).
- Ginalski, K., Elofsson, A., Fischer, D. & Rychlewski, L. 3D-Jury: a simple approach to improve protein structure predictions. *Bioinformatics* **19**, 1015–1018 (2003).
- Arcus, V. OB-fold domains: a snapshot of the evolution of sequence, structure and function. *Curr. Opin. Struct. Biol.* **12**, 794–801 (2002).
- Theobald, D.L., Mitton-Fry, R.M. & Wuttke, D.S. Nucleic acid recognition by OB-fold proteins. *Annu. Rev. Biophys. Biomol. Struct.* **32**, 115–133 (2003).
- Theobald, D.L. & Wuttke, D.S. Divergent evolution within protein superfolds inferred from profile-based phylogenetics. *J. Mol. Biol.* **354**, 722–737 (2005).
- Santocanale, C., Neeck, H., Longhese, M.P., Lucchini, G. & Plevani, P. Mutations in the gene encoding the 34 kDa subunit of yeast Replication Protein A cause defective S phase progression. *J. Mol. Biol.* **254**, 595–607 (1995).
- Philipova, D. *et al.* A hierarchy of SSB protomers in Replication Protein A. *Genes Dev.* **10**, 2222–2233 (1996).
- Maniar, H.S., Wilson, R. & Brill, S.J. Roles of replication protein-A subunits 2 and 3 in DNA replication fork movement in *Saccharomyces cerevisiae*. *Genetics* **145**, 891–902 (1997).
- Mitton-Fry, R.M., Anderson, E.M., Hughes, T.R., Lundblad, V. & Wuttke, D.S. Conserved structure for single-stranded telomeric DNA recognition. *Science* **296**, 145–147 (2002).
- Sibenaller, Z.A., Sorensen, B.R. & Wold, M.S. The 32- and 14-kilodalton subunits of Replication Protein A are responsible for species-specific interactions with single-stranded DNA. *Biochemistry* **37**, 12496–12506 (1998).
- Bochkareva, E., Frappier, L., Edwards, A.M. & Bochkarev, A. The RPA32 subunit of human Replication Protein A contains a single-stranded DNA-binding domain. *J. Biol. Chem.* **273**, 3932–3936 (1998).
- Lin, Y.L., Chen, C., Keshav, K.F., Winchester, E. & Dutta, A. Dissection of functional domains of the human DNA replication protein complex Replication Protein A. *J. Biol. Chem.* **271**, 17190–17198 (1996).
- Venclovas, C. & Thelen, M.P. Structure-based predictions of Rad1, Rad9, Hus1 and Rad17 complex in sliding clamp and clamp-loading complexes. *Nucleic Acids Res.* **28**, 2481–2493 (2000).
- Green, C.M., Erdjument-Bromage, H., Tempst, P. & Lowndes, N.F. A novel Rad24 checkpoint protein complex closely related to replication factor C. *Curr. Biol.* **10**, 39–42 (2000).
- Paarrilla-Castellar, E.R., Arlander, S.J. & Karnitz, L. Dial 9–1-1 for DNA damage: the Rad9-Hus1-Rad1 (9–1-1) clamp complex. *DNA Repair (Amst.)* **3**, 1009–1014 (2004).
- Aroya, S.B. & Kupiec, M. The Elg1 replication factor C-like complex: a novel guardian of genome stability. *DNA Repair (Amst.)* **4**, 409–417 (2005).
- Wold, M.S., Weinberg, D.H., Virshup, D.M., Li, J.J. & Kelly, T.J. Identification of cellular proteins required for simian virus 40 DNA replication. *J. Biol. Chem.* **264**, 2801–2809 (1989).
- Bochkareva, E., Belegu, V., Korolev, S. & Bochkarev, A. Structure of the major single-stranded DNA-binding domain of Replication Protein A suggests a dynamic mechanism for DNA binding. *EMBO J.* **20**, 612–618 (2001).
- Theobald, D.L. & Wuttke, D.S. Prediction of multiple tandem OB-fold domains in telomere end-binding proteins Pot1 and Cdc13. *Structure* **12**, 1877–1879 (2004).
- Zou, L. & Elledge, S.J. Sensing DNA damage through ATRIP recognition of RPA-ssDNA complexes. *Science* **300**, 1542–1548 (2003).
- Lisby, M., Barlow, J.H., Burgess, R.C. & Rothstein, R. Choreography of the DNA damage response: spatiotemporal relationships among checkpoint and repair proteins. *Cell* **118**, 699–713 (2004).
- Wellinger, R.J., Wolf, A.J. & Zakian, V.A. *Saccharomyces cerevisiae* telomeres acquire single-strand TG₁₋₃ tails late in S phase. *Cell* **72**, 51–60 (1993).
- Wellinger, R.J., Ethier, K., Labrecque, P. & Zakian, V.A. Evidence for a new step in telomere maintenance. *Cell* **85**, 423–433 (1996).
- Takata, H., Kanoh, Y., Gunge, N., Shirahige, K. & Matsuur, A. Reciprocal association of the budding yeast ATM-related proteins Tel1 and Mec1 with telomeres *in vivo*. *Mol. Cell* **14**, 515–522 (2004).
- Smith, J., Zou, H. & Rothstein, R. Characterization of genetic interactions with *RFA1*: the role of RPA in DNA replication and telomere maintenance. *Biochimie* **82**, 71–78 (2000).
- Schramke, V. *et al.* RPA regulates telomerase action by providing Est1p access to chromosome ends. *Nat. Genet.* **36**, 46–54 (2004).
- Altschul, S.F. *et al.* Gapped BLAST and PSI-BLAST: a new generation of protein database search programs. *Nucleic Acids Res.* **25**, 3389–3402 (1997).
- Eddy, S.R. Profile hidden Markov models. *Bioinformatics* **14**, 755–763 (1998).
- Poirot, O., O'Toole, E. & Notredame, C. Tcoffee@igs: A web server for computing, evaluating and combining multiple sequence alignments. *Nucleic Acids Res.* **31**, 3503–3506 (2003).
- Poirot, O., Suhre, K., Abergel, C., O'Toole, E. & Notredame, C. 3DCoffee@igs: a web server for combining sequences and structures into a multiple sequence alignment. *Nucleic Acids Res.* **32**, W37–W40 (2004).
- Do, C.B., Mahabhashyam, M.S., Brudno, M. & Batzoglou, S. ProbCons: Probabilistic consistency-based multiple sequence alignment. *Genome Res.* **15**, 330–340 (2005).

